Article

# Excited State Intervalence Transfer in a Rigid Polymeric Film

Cavan N. Fleming, Dana M. Dattelbaum, David W. Thompson, Aleksei Yu. Ershov, and Thomas J. Meyer

*J. Am. Chem. Soc.*, **2007**, 129 (31), 9622-9630• DOI: 10.1021/ja068074j • Publication Date (Web): 14 July 2007



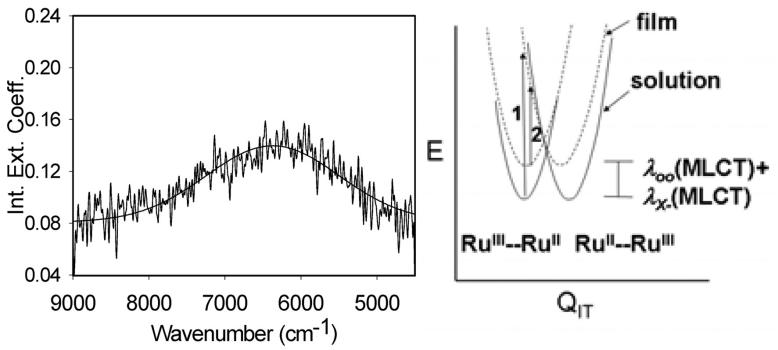


## More About This Article

Additional resources and features associated with this article are available within the HTML version:

- Supporting Information
- Links to the 1 articles that cite this article, as of the time of this article download
- Access to high resolution figures
- Links to articles and content related to this article
- Copyright permission to reproduce figures and/or text from this article

View the Full Text HTML

J|A|C|S
ARTICLES
Published on Web 07/14/2007

# Excited State Intervalence Transfer in a Rigid Polymeric Film

Cavan N. Fleming,[†] Dana M. Dattelbaum,*[,‡] David W. Thompson,[†,||] Aleksei Yu. Ershov,[§] and Thomas J. Meyer*[,†]

*Contribution from the Department of Chemistry, University of North Carolina, Chapel Hill, North Carolina 27599, Los Alamos National Laboratory, MS P952, Los Alamos, New Mexico 87545, and Institute of Chemistry of St. Petersburg State University, St. Petersburg 198904, Russia*

Received December 11, 2006; E-mail: danadat@lanl.gov; tjmeyer@unc.edu

***Abstract:*** The ligand-bridged complex *cis,cis*-$[(bpy)_2ClRu(pz)RuCl(bpy)_2]^{2+}$ as the $PF_6^-$ salt, (**1**)$(PF_6)_2$, is stabilized toward photochemical ligand loss in poly(methyl methacrylate) (PMMA). Stabilization allows measurement of metal-to-ligand charge transfer (MLCT) photophysical properties—emission and transient absorption. This includes appearance of an intervalence transfer absorption band in the near IR spectrum of the photochemically prepared, mixed valence form, $[(bpy)_2ClRu^{III}(pz^{-\bullet})Ru^{II}Cl(bpy)_2](PF_6)_2$* (**1***$(PF_6)_2$). Comparison of its IT band properties with those of ground state *cis,cis*-$(bpy)_2ClRu^{III}(pz)Ru^{II}Cl(bpy)_2]^{3+}$ in $CD_3CN$ allows a comparison to be made between pz and $pz^{-\bullet}$ as bridging ligands. A model based on differences between rigid and fluid media provides an explanation for decreased IT band energies and widths in PMMA and provides important insight into electron transfer in rigid media.

## Introduction

Light absorption by $Ru^{II}$ polypyridyl complexes in the visible region is dominated by spin-allowed metal-to-ligand charge transfer (MLCT) absorption bands which, upon excitation, give excited states largely singlet in character ($^1$MLCT). Emission occurs from the corresponding triplet states, $^3$MLCT, and occurs at lower energy.[1] The excited singlet and triplet states are mixed by spin−orbit coupling with $\zeta(Ru^{III}) \sim 1000$ cm$^{-1}$.

There are also low-lying metal-centered "dd" states in the excited-state manifolds. Following MLCT excitation and thermal equilibration, they are populated by thermally-activated surface crossing, $^3(d\pi_{Ru}{}^5\pi^*_{bpy}{}^1) \rightarrow d\pi_{Ru}{}^5\, d\sigma_{Ru}{}^*$. The orbital labels $d\pi$ and $d\sigma^*$ refer to the $t_{2g}$ and $e_g$ orbitals of $O_h$ symmetry.

Once formed in solution, dd states are short-lived and the cause of ligand-loss photochemistry.[2] Their appearance in excited-state manifolds greatly limits the use of certain types of $Ru^{II}$ polypyridyl complexes as building blocks for the study of photoinduced electron and energy transfer in solution. A number of strategies have evolved for minimizing their deleterious effects. With an appropriate combination of ligands, the dd-MLCT energy gap can be increased, increasing the MLCT → dd barrier.[3] A second strategy utilizes rigid media such as cellulose acetate,[4] poly(ethylene oxide),[5] zeolites,[6] poly(methyl methacrylate) (PMMA), and $SiO_2$ sol−gel monoliths which stabilize polypyridyl complexes toward ligand loss.[7] Temperature-dependent lifetime measurements in these media reveal that dd-state reactivity is greatly inhibited, decreasing or even eliminating ligand-loss photochemistry. Electron transfer, which can be decreased or completely inhibited in rigid media, can continue to occur if proper attention is paid to the impact of the medium on the free energy change.[8]

[†] The University of North Carolina.
[‡] Los Alamos National Laboratory.
[§] Institute of Chemistry of St. Petersburg State University.
[||] Present address: Department of Chemistry, Memorial University of Newfoundland, St. John's NL, A1B 3X7, Canada.

(1) (a) Damrauer, N. H.; Cerullo, G.; Yeh, A.; Boussie, T. R.; Shank, C. V.; McCusker, J. K. *Science* **1997**, *275*, 54. (b) Demas, J. N.; Crosby, G. A. *J. Am. Chem. Soc.* **1971**, *93*, 2841. (c) Hager, G. D.; Crosby, G. A. *J. Am. Chem. Soc.* **1975**, *97*, 7031. (d) Lumpkin, R. S.; Kober, E. M.; Worl, L. A.; Murtaza, Z.; Meyer, T. J. *J. Phys. Chem.* **1990**, *94*, 239. (e) Kober, E. M.; Meyer, T. J. *Inorg. Chem.* **1984**, *23*, 3877. (f.) Meyer, T. J. *Pure Appl. Chem.* **1986**, *58*, 1193. (g) Juris, A.; Balzani, V.; Barigelletti, F.; Campagna, S.; Beleser, P.; von Zelewsky, A. *Coord. Chem. Rev.* **1988**, *84*, 85. (h) Brennamen, M. K.; Alstrum-Acevedo, J. H.; Fleming, C. N.; Jang, P.; Meyer, T. J.; Papanikolas, J. M. *J. Am. Chem. Soc.* **2002**, *124*, 15094. (i) Brennamen, M. K.; Meyer, T. J.; Papanikolas, J. *J. Phys. Chem. A* **2004**, *108*, 9938. (j) McCusker, J. K. *Acc. Chem. Res.* **2003**, *36*, 876.

(2) (a) Durham, B.; Caspar, J. V.; Nagle, J. K.; Meyer, T. J. *J. Am. Chem. Soc.* **1982**, *104*, 4803 (b) Van Houten, J.; Watts, R. J. *J. Am. Chem. Soc.* **1976**, *98*, 4853. (c) Van Houten, J.; Watts, R. J. *Inorg. Chem.* **1978**, *17*, 3381. (d) Kirchhoff, J. R.; McMillin, D. R.; Marnot, P. A.; Sauvage, J. *J. Am. Chem. Soc.* **1985**, *107*, 1138. (e) Hecker, C. R.; Gushurst, A. K. I.; McMillin, D. R. *Inorg. Chem.* **1991**, *30*, 538. (f) Islam, A.; Ikeda, N.; Yoshimura, A.; Ohno, T. *Inorg. Chem.* **1998**, *37*, 3093. (g) Islam, A.; Ikeda, N.; Nozaki, K.; Ohno, T. *Chem. Phys. Lett.* **1996**, *263I*, 209. (h) Macatangay, A.; Zheng, G. Y.; Rillema, D. P.; Jackman, D. C.; Merkert, J. W. *Inorg. Chem.* **1996**, *35*, 6823. (i) Thompson, D. W.; Wishart, J. F.; Brunschwig, B. S.; Sutin, N. *J. Phys. Chem. A* **2001**, *105*, 8117. (j) Draxler, S. *J. Phys. Chem. A* **1999**, *103*, 4719. (k) Coe. B. J.; Thompson, D. W.; Culbertson, C. D.; Schoonover, J. R.; Meyer, T. J. *Inorg. Chem.* **1995**, *34*, 3385. (l) Winkler, J. R.; Netzel, T. L.; Creutz, C.; Sutin, N. *J. Am. Chem. Soc.* **1987**, *109*, 2381. (m) Benniston, A. C.; Chapman, G.; Harriman, A.; Mehrabi, M.; Sams, C. A. *Inorg. Chem.* **2004**, *43*, 4227.

(3) (a) Allen, G. H.; White, R. P.; Rillema, D. P.; Meyer, T. J. *J. Am. Chem. Soc.* **1984**, *106*, 2613. (b) Caspar, J. V.; Meyer, T. J. *Inorg. Chem.* **1983**, *22*, 2444. (c) Cherry, W. R.; Henderson, L. J. *Inorg. Chem.* **1984**, *23*, 983. (d) Wacholtz, W. F.; Auerbach, R. A.; Schmehl, R. H. *Inorg. Chem.* **1986**, *25*, 227.

(4) Allsopp, S. R.; Cox, A.; Kemp, T. J.; Reed, W. J. *J. Chem. Soc., Faraday Trans.* **1978**, *74*, 1275.

(5) Campagna, S.; Bartolotta, A.; Di Marco, G. *Chem. Phys. Lett.* **1993**, *206*, 30.

(6) Maruszewski, K.; Strommen, D. P.; Kincaid, J. R. *J. Am. Chem. Soc.* **1993**, *115*, 8345.

(7) Adelt, M.; Devenney, M.; Meyer, T. J.; Thompson, D. W.; Treadway, J. A. *Inorg. Chem.* **1998**, *37*, 2616. Pinnick, D. V.; Durham, B. *Inorg. Chem.* **1984**, *23*, 1440.

 **10.1021/ja068074j CCC: $37.00** 

As part of a long-term goal of designing and understanding efficient light-driven molecular processes in device-like environments, we are exploring the use of rigid media to stabilize molecular assemblies that are photochemically unstable in solution. We are also interested in understanding, in a systematic way, the photochemical and photophysical properties of molecules and molecular assemblies in these media.

With those goals in mind we report here the results of a transient near IR study on the salt *cis,cis*-$[(bpy)_2ClRu(pz)RuCl(bpy)_2](PF_6)_2$ (**1**$(PF_6)_2$) immobilized in thin, optically transparent films of PMMA. (The repeat structure of PMMA is illustrated below.)

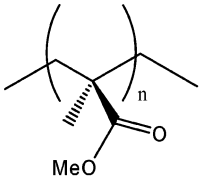


Poly(methylmethacrylate) (*PMMA*)

In solution, this complex is highly unstable toward photochemical ligand loss. Stabilization in PMMA has allowed us to investigate the photophysical properties of its lowest energy, pz-based, mixed-valence, MLCT excited state, $[(bpy)_2ClRu^{III}(pz^{-\bullet})Ru^{II}Cl(bpy)_2]^{2+}$*. This includes observation of a $Ru^{II} \rightarrow Ru^{III}$ intervalence transfer (IT) band associated with the excited-state complex, the second observation of its kind.[18] Comparisons with the IT band for ground state $[(bpy)_2ClRu^{III}(pz)Ru^{II}Cl(bpy)_2]^{3+}$ in $CD_3CN$ show that pz and $pz^{-\bullet}$ have comparable abilities in promoting electronic coupling between $Ru^{III}$ and $Ru^{II}$ in this coordination environment. A shift of the IT band to lower energy in PMMA is a consequence of its rigid character and has important implications for electron transfer in rigid media.

## Experimental Section

**Materials.** Medium molecular weight ($\overline{MW}$ ~350 000) poly(methylmethacrylate) (PMMA) was purchased from Aldrich. A weakly emitting impurity at ~510 nm appeared following 460 nm excitation. It was removed by Soxhlet extraction with benzene followed by multiple precipitations of the polymer from methanol solution. Chloroform and acetonitrile were purchased from Burdick and Jackson and used as received. The salt *cis,cis*-$[(bpy)_2ClRu(pz)RuCl(bpy)_2](PF_6)_2$ (**1**) was synthesized as described elsewhere.[9] The salt *cis*-$[Ru(bpy)_2(pz)Cl](PF_6)$ (**2**) was synthesized by a modification of a previously described procedure.[10]

**Preparation of Polymer Films.** A 0.5 g amount of PMMA was dissolved in 5 mL of chloroform. The resulting solution was added to 1 mL of acetonitrile containing the complex, stirred, and poured into a Teflon mold. The solvent was allowed to evaporate slowly over a period of 2−3 days in a desiccator held at ambient temperature. The resulting film was placed in a vacuum desiccator for 2 days prior to making measurements. The films produced were 4 cm in length and 1 cm in width and had a fairly uniform thickness of ~0.8 mm.

**Measurements.** Steady-state emission spectra were recorded on a SPEX Fluorolog-212 spectrofluorimeter with right angle geometry, corrected for the instrument response. Photolysis measurements were conducted by passing light from a 200 W Hg lamp through a Bausch and Lomb monochromator. The excitation beam was directed through UV and IR cutoff filters prior to entering the film. UV−visible absorption spectra were recorded on an HP 8451-A diode array spectrophotometer. Emission lifetimes were obtained, following 460 nm excitation at 100 $\mu$J/pulse, with a PRA grating LN102/1000 tunable dye laser pumped at 337 nm by a PRA LN1000 pulsed nitrogen laser in a system described more completely elsewhere.[11] The excited-state absorption measurements were conducted by using a Continuum Surelite II-10 Nd:YAG-OPO laser system as the pump and a 250 W pulsed Xe lamp as the probe in a system also described in more detail elsewhere.[12] The films scattered light, and a variety of bandpass and cutoff filters and two pump wavelengths (460 and 500 nm) were used to collect full spectra.

**Time-Resolved Near-Infrared Spectroscopy (TRNIR).** Measurements in the near-IR region were made on a modified step-scan FTIR instrument. The instrument was a Bruker IFS 66V/s step-scan FTIR spectrometer with a near IR (tungsten) source and a Quartz I beamsplitter. In the experiment, the sample was excited with a pump beam at 510 nm from the Continuum Surelite Nd:YAG OPO combination mentioned above. The transients produced were probed with broad band NIR light with detection by a liquid $N_2$-cooled mercury−cadmium−telluride (MCT) detector containing a face-mounted bandpass filter. The filter limited the spectral observation region to 2600−8400 $cm^{-1}$. The details of the step-scan experiment have been described elsewhere.[13] The complex-doped PMMA film was mounted at the focal point of both pump and probe beams.

Due to the lack of available actinometers in the near IR, $\epsilon_{max}$ for **1*** was estimated by using the energy per photon ($3.6 \times 10^{-19}$ J), the number of photons per pulse (pulse energy = 510 $\mu$J/pulse, $1.38 \times 10^{15}$ photons/pulse), and the fraction of light absorbed by the sample ($\phi = 1 - T$; $T = 10^{-\epsilon bc}$ from Beer's Law, $\epsilon_{510} = 2.6 \times 10^4$ $M^{-1}$ $cm^{-1}$) to give the number of photons absorbed by the sample. This quantity was converted into the number of moles excited and divided by the excitation volume to calculate the concentration of the excited states. An additional correction was made to correlate the time-resolved infrared signal intensity with that observed by transient emission. The first detectable transient signal from the excited state in the infrared experiment was ~30 ns after excitation by the pump beam. This is

(8) (a) Jones, W. E.; Chen, P.; Meyer, T. J. *J. Am. Chem. Soc.* **1992**, *114*, 387. (b) Chen, P.; Danielson, E.; Meyer, T. J. *J. Phys. Chem.* **1988**, *92*, 3708.
(9) (a) Callahan, R. W.; Keene, F. R.; Meyer, T. J.; Salmon, D. J. *J. Am. Chem. Soc.* **1977**, *99*, 1064. (b) Powers, M. J.; Meyer, T. J. *J. Am. Chem. Soc.* **1980**, *102*, 1289.
(10) Adeyemi, S. A.; Johnson, E. C.; Miller, F. J.; Meyer, T. J. *Inorg. Chem.* **1973**, *12*, 2371.
(11) Devenney, M.; Worl, L. A.; Gould, S.; Guadalupe, A.; Sullivan, B. P.; Casper, J. V.; Leasure, R. L.; Gardner, J. R.; Meyer, T. J. *J. Phys. Chem. A* **1997**, *101*, 4535.
(12) Maxwell, K. A.; Sykora, M.; DeSimone, J. M.; Meyer, T. J. *Inorg. Chem.* **2000**, *39*, 71−75.
(13) Dattelbaum, D. M.; Omberg, K. M.; Schoonover, J. R.; Martin, R. L.; Meyer, T. J. *Inorg. Chem.* **2002**, *41*, 6071−6079.
(14) Veletsky, N. I.; Dementiev, I. A.; Ershov, A. Y.; Nikol'skii; A. B. *J. Photochem. Photobiol. A* **1995**, *89*, 99.
(15) Thompson, D. W.; Fleming, C. N.; Myron, C. D.; Meyer, T. J. *J. Phys. Chem. B* **2007**, *111*, 6930−6941. Adelt, M.; Devenney, M.; Meyer, T. J.; Thompson, D. W.; Treadway, J. A. *Inorg. Chem.* **1998**, *37*, 2616.
(16) Creutz, C.; Chou, M.; Netzel, T. L.; Okumura, M.; Sutin, N. *J. Am. Chem. Soc.* **1980**, *102*, 1309.
(17) (a) Williams, G.; Watts, D. C. *Trans. Faraday Soc.* **1970**, *66*, 80. (b) Lindsey, C. P.; Patterson, G. D. *J. Chem. Phys.* **1980**, *73*, 3348. (c) The nonexponential decay kinetics may reflect a kinetic coupling of the emissive $^3$MLCT and low-lying dd states which give rise to photodecomposition in fluid media. This behavior has been observed for *cis*-$[Ru(bpy)_2(py)_2]^{2+}$* in PMMA and is discussed in detail elsewhere.[15] A full analysis of the kinetic coupling mechanism requires temperature-dependent lifetime data and is outside the scope of this study.
(18) Dattelbaum, D. M.; Hartshorn, C. M.; Meyer, T. J. *J. Am. Chem. Soc.* **2002**, *124* (18), 4938−4939.
(19) Dattelbaum, D. M.; Kober, E. M.; Papanikolas, J. M.; Meyer, T. J. *Chem. Phys.* **2006**, *326*, 71−78.
(20) (a) Plummer, E. A.; Zink, J. I. *Inorg. Chem.* **2006**, *45*, 6556−6558. Lockard, J. V.; Zink, J. I.; Konradsson, A. E.; Weaver, M. N.; Nelsen, S. F. *J. Am. Chem. Soc.* **2003**, *125*, 13471−13480. Nelsen, S. F.; Konradsson, A. E.; Weaver, M. N.; Guzei, I. A.; Goebel, M.; Wortmann, R.; Lockard, J. V.; Zink, J. I. *J. Phys. Chem.* **2005**, *109*, 10854−10861. Lockard, J. V.; Zink, J. I.; Trieber, D. A.; Konradsson, A. E.; Weaver, M. N.; Nelsen, S. F. *J. Phys. Chem. A* **2005**, *109*, 1205−1215. (b) Bignozzi, C. A.; Argazzi, R.; Chiorboli, C.; Scandola, F.; Dyer, R. B.; Schoonover, J. R.; Meyer, T. J. *Inorg. Chem.* **1994**, *33*, 1652−1659. Bignozzi, C. A.; Argazzi, R.; Schoonover, J. R.; Gordon, K. C.; Dyer, R. B.; Scandola, F. *Inorg. Chem.* **2002**, *31*, 5260−5267.

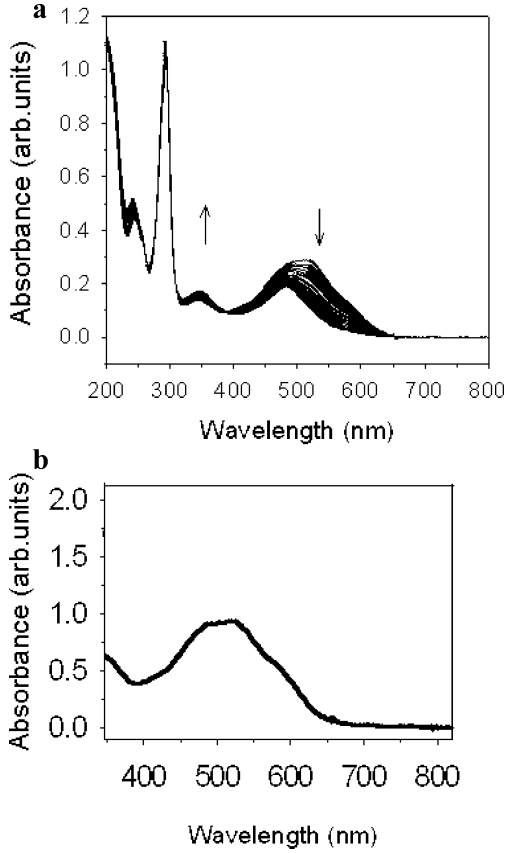


***Figure 1.*** (a) UV/visible absorption spectral changes upon photolysis of *cis,cis*-[(bpy)$_2$ClRu(pz)RuCl(bpy)$_2$](PF$_6$)$_2$ in CH$_3$CN at 460 nm. The limiting spectrum of *cis*-[Ru(bpy)$_2$Cl(CH$_3$CN)]$^+$ was obtained after 100 min of photolysis. (b) UV/visible absorption spectra of *cis,cis*-[(bpy)$_2$ClRu(pz)-RuCl(bpy)$_2$](PF$_6$)$_2$ in PMMA before and after 460 nm photolysis under the same conditions.

due to the rise time of the infrared detector (25 ns). After 30 ns, there is an ~27% luminescence intensity loss by transient emission. ΔOD was corrected for the rise time of the infrared detector based on transient emission measurements on the same film. With ΔOD, the calculated excited-state concentration, and $b = 0.8$ mm, $\epsilon_{max} \approx 970$ M$^{-1}$ cm$^{-1}$ at 6880 cm$^{-1}$. This is an upper limit since it assumes unit efficiency of formation of **1***(PF$_6$)$_2$. There is a negligible absorption by the ground state in the near-infrared region.

## Results and Discussion

The complex *cis,cis*-[(bpy)$_2$ClRu(pz)RuCl(bpy)$_2$]$^{2+}$ (**1**) is extremely light sensitive in solution, undergoing stepwise ligand loss and decomposition, eq 1. Spectral changes with time (Figure 1a) occur with isosbestic points at 400 and 375 nm consistent with formation of *cis*-[Ru(bpy)$_2$(pz)Cl]$^+$ and *cis*-[Ru(bpy)$_2$(CH$_3$-CN)Cl]$^+$ with the latter as the ultimate photoproduct. The quantum yield for the step in eq 1b is $\Phi = 0.26$.[14] The complex is stable indefinitely in solution in the absence of light.

$$[(bpy)_2ClRu(pz)RuCl(bpy)_2]^{2+} + CH_3CN \xrightarrow[\Phi_1]{h\nu} [Ru(bpy)_2(pz)Cl]^+ + [Ru(bpy)_2(CH_3CN)Cl]^+ \quad (1a)$$

$$[Ru(bpy)_2(pz)Cl]^+ + CH_3CN \xrightarrow{h\nu} [Ru(bpy)_2(CH_3CN)Cl]^+ + pz \quad (1b)$$

By contrast, in rigid poly(methylmethacrylate) (PMMA) there is no sign of photodecomposition of *cis,cis*-[(bpy)$_2$ClRu(pz)-RuCl(bpy)$_2$](PF$_6$)$_2$ (**1**(PF$_6$)$_2$) under comparable conditions (Figure 1b). The rigid nature of the film stabilizes the complex toward ligand loss by inhibiting large amplitude motions associated with metal−ligand bond breaking in the dd state(s). It also creates a local "cage effect" inhibiting translational separation of the photoproducts which promotes recoordination of a ligand once released.[15]

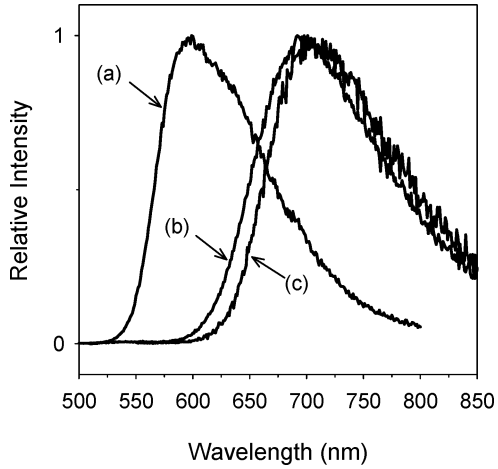


***Figure 2.*** Normalized emission spectra for [Ru(bpy)$_3$](PF$_6$)$_2$ (a), *cis*-[Ru-(bpy)$_2$(pz)Cl](PF$_6$) (b), and *cis,cis*-[(bpy)$_2$ClRu(pz)RuCl(bpy)$_2$](PF$_6$)$_2$ (c) all in PMMA following 460 nm excitation at room temperature.

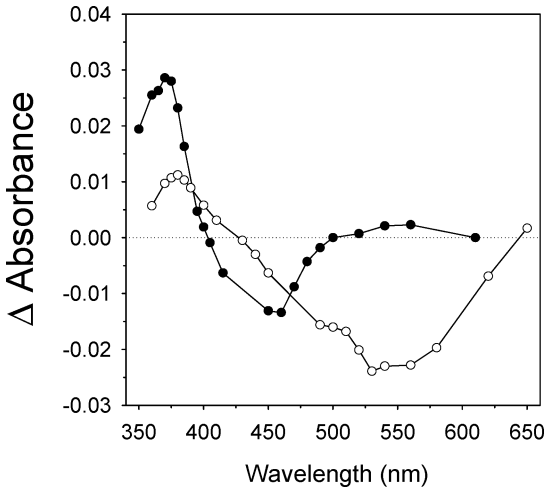


***Figure 3.*** Excited-state transient absorption difference spectra for *cis,cis*-[(bpy)$_2$ClRu(pz)RuCl(bpy)$_2$](PF$_6$)$_2$ (○) and [Ru(bpy)$_3$](PF$_6$)$_2$ (●) in PMMA at room temperature. The spectra were obtained following excitation at either 460 or 500 nm with 2.5 mJ/pulse.

Rigid medium stabilization has allowed us to explore the photophysical properties of (**1**)(PF$_6$)$_2$. The absorption band at 520 nm in Figure 1 is d$\pi$(Ru$^{II}$) → $\pi$*(pz) in origin, and the shoulder at ~480 nm, d$\pi$(Ru$^{II}$) → $\pi$*(bpy).[9] As shown in Figure 2c, d$\pi$(Ru$^{III}$)−$\pi$*(pz$^{-\bullet}$) emission from (**1***)(PF$_6$)$_2$ occurs at $\lambda_{max}$ = 725 nm. MLCT-based emissions from [Ru(bpy)$_3$](PF$_6$)$_2$* (Figure 2a) and *cis*-[Ru(bpy)$_2$(pz)Cl](PF$_6$)* (Figure 2b) in PMMA are also shown for comparison.

Transient absorption difference spectra for (**1**)(PF$_6$)$_2$ (○) and [Ru(bpy)$_3$](PF$_6$)$_2$ (●) in PMMA are shown in Figure 3. The positive features at <400 nm originate from ligand-centered $\pi$* → $\pi$* bands on the partly reduced acceptor ligand.[16] For the pz-based excited state this feature is centered at 380 nm and is a factor of ~2 less intense than the ground state bleach at 530 nm. The ground state bleach coincides with the known d$\pi$ →

$\pi^*$(pz) absorption at 530 nm.[9] By comparison, ligand-centered absorption in $[Ru(bpy)_3](PF_6)_2$* appears at 370 nm and is more intense by a factor of ~2 than the bleach at ~450 nm. The appearance of the bleach at ~530 nm for **1***$(PF_6)_2$ is consistent with loss of the $Ru^{II} \rightarrow$ pz absorption in the excited state, Figure 1, with pz as the acceptor ligand.

Excited-state decays in PMMA for both **1***$(PF_6)_2$ and *cis*-$[Ru(bpy)_2(pz)Cl](PF_6)$* (**2***$(PF_6)$) are complex. They were fit to the Williams−Watts function in eq 2 in which $\beta$ is the distribution width, a measure of deviation from exponentiality.[17b] The average lifetime, $\langle\tau\rangle$, was calculated from eq 3a,

$$I(t) = I_0 \exp -(k_1 t)^{\beta} \tag{2}$$

$$\langle\tau\rangle = (k_1\beta)^{-1}\cdot\Gamma(1/\beta) \tag{3a}$$

with the gamma function, $\Gamma(n)$, defined in eq 3b.

$$\Gamma(n) = \int_0^{\infty} x^{n-1}\, e^{-x}\, \mathrm{d}x = \frac{1}{n}\prod_{m=1}^{\infty}\frac{\left(1+\frac{1}{m}\right)^n}{1+\frac{n}{m}} \tag{3b}$$

Analysis of emission decay for **1***$(PF_6)_2$ at room temperature with monitoring at 700 nm gave $\beta = 0.60$ and $\langle\tau\rangle = 100$ ns. For **2***, $\beta = 0.46$ and $\langle\tau\rangle = 70$ ns. By contrast, decay from $[Ru(bpy)_3](PF_6)_2$* is more nearly exponential with $\beta = 0.90$ and $\langle\tau\rangle = 1420$ ns. The broader distributions for the complexes with pyrazine as the acceptor ligand is a feature shared by *cis*-$[Ru(bpy)_2(py)_2](PF_6)_2$ in PMMA. It has been attributed to the reversible, dynamic involvement of a low-lying dd state or states in nonradiative decay.[15,17c]

**Excited State Intervalence Transfer.** The results of the transient absorption and emission measurements are consistent with a $\pi^*$(pz)-based MLCT excited state as the transient observed following $d\pi(Ru^{II}) \rightarrow \pi^*$(bpy), $\pi^*$(pz) MLCT excitation. Assuming localized oxidation states, photoexcitation creates a mixed valence excited state as shown in eq 4. The appearance of this state introduces the possibility of observing an excited state IT band or bands by using the transient IR−near-IR apparatus described above. This apparatus was used previously to observe an excited state IT band in a related complex in solution[18] and, more recently, to observe a ligand-to-ligand charge-transfer band (LLCT) in the MLCT excited state of $[Os(phen)_3]^{2+}$.[19] Evidence for ligand-based IT bands in mixed valence excited states has been reported by Zink and coworkers.[20a] The transient IR technique has also been applied to mixed-valence excited states by observing shifts in $\nu$(CO) and $\nu$(CN) vibrations.[20b]

$$[(bpy)_2(Cl)Ru^{II}(pz)Ru^{II}(Cl)(bpy)_2](PF_6)_2 \xrightarrow{h\nu} [(bpy)_2(Cl)Ru^{III}(pz^{\bullet-})Ru^{II}(Cl)(bpy)_2](PF_6)_2^* \tag{4}$$

The transient near-infrared (TRNIR) spectrum of **1***$(PF_6)_2$ in PMMA is shown in Figure 4B. It was acquired by near-infrared monitoring following visible laser flash excitation. The nonzero baseline is an experimental artifact arising from difficulties in subtracting differences arising from intense overtones at ~8520 and 7188 $cm^{-1}$.

The spectrum in Figure 4B shows the appearance of a transient absorption feature at $\bar{\nu}_{max} = 6880$ $cm^{-1}$ with $\Delta\bar{\nu}_{1/2} =$ 3740 $cm^{-1}$ and $\epsilon_{max} \geq 970$ $M^{-1}$ $cm^{-1}$.[21] The spectrum is shown in Figure 4C rescaled as $\int \epsilon(\nu)\, \mathrm{d}\ln\nu$ which is directly related to the transition moment, eq 5.

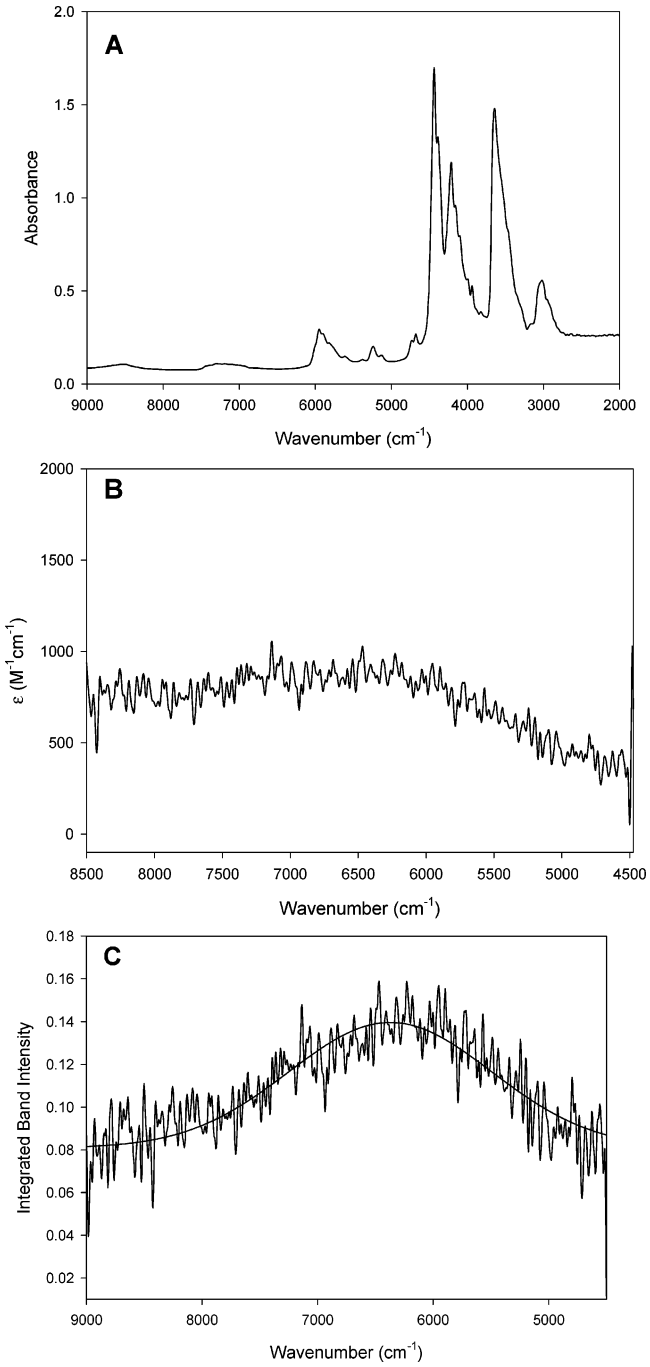


***Figure 4.*** (A) Ground-state spectrum of $[(bpy)_2(Cl)Ru(pz)Ru(Cl)(bpy)_2](PF_6)_2$ in PMMA at 298 K. (B) TRNIR difference spectra for $[(bpy)_2(Cl)Ru(pz)Ru(Cl)(bpy)_2](PF_6)_2$ in PMMA at 298 K following 510 nm excitation (175 $\mu$J/pulse). For the transient IT feature, $\bar{\nu}_{max} = 6880$ $cm^{-1}$, and $\Delta\bar{\nu}_{1/2} = 3740$ $cm^{-1}$. (C) The spectrum in (B) rescaled as $\int \epsilon(\nu)\, \mathrm{d}\ln\nu$ vs $\bar{\nu}$ for $[(bpy)_2(Cl)Ru(pz)Ru(Cl)(bpy)_2]^*(PF_6)_2$ with $\bar{\nu}_{max} = 6370$ $cm^{-1}$ and $\Delta\bar{\nu}_{1/2} = 2060$ $cm^{-1}$ for the transient.

$$|\vec{M}|^2 = \frac{3000cn\hbar\ln 10}{4\pi^2 N_A}\int \epsilon(\nu)\, \mathrm{d}\ln\nu \tag{5}$$

In eq 5, $n$ is the index of refraction (1.34 for $CH_3CN$), $c$ is the speed of light ($3.00 \times 10^8$ m/s), $N_A$ is Avogadro's constant (6.02

$\times 10^{23}$), and $\hbar$ is $h/2\pi$ ($1.06 \times 10^{-34}$ J s, $5.31 \times 10^{-12}$ cm$^{-1}$ s). $\epsilon(\nu)$ is the molar extinction coefficient at frequency $\nu$. For the rescaled spectrum, $\bar{\nu}_{max} = 6370$ cm$^{-1}$, $\epsilon_{max} \geq 970$ M$^{-1}$ cm$^{-1}$,[20] $\Delta\bar{\nu}_{1/2} = 2060$ cm$^{-1}$, and $\int \epsilon(\nu)\, d \ln \nu \geq 2.0 \times 10^6$. With the excited-state band shape parameters and eq 5, $\vec{M} \geq 0.014$ Å.

**Analysis of IT Bands.** The electron-transfer matrix element, $H_{DA}$, the resonance energy arising from electronic wavefunction mixing between the donor and acceptor, can also be calculated from eq 6a and, for a Gaussian shaped band, from eq 6b. In these equations $d$ is the internuclear, Ru−Ru separation distance, and $e$, the unit electron charge.

Contributing to the inequality in eq 6 is the fact that the charge-transfer distance is less than the geometrical distance in these complexes due to electronic delocalization.[22] Based on eq 6 and $\vec{M} \geq 0.014$ Å, $H_{DA} \geq 340$ cm$^{-1}$ for **1***$(PF_6)_2$ with $\vec{M}$ as the transition moment.

$$H_{DA} \geq \frac{M\bar{\nu}_{max}}{ed} \tag{6a}$$

$$H_{DA} \geq \left(\frac{(4.2 \times 10^{-4})\epsilon_{max}\Delta\bar{\nu}_{1/2}\bar{\nu}_{max}}{d^2}\right)^{1/2} \tag{6b}$$

For the ground state mixed-valence ion, *cis*,*cis*-$[(bpy)_2ClRu^{III}(pz)Ru^{II}Cl(bpy)_2]^{3+}$ in $CD_3CN$ at 298 K, an IT band appears at $\bar{\nu}_{max} = 7700$ cm$^{-1}$ with $\Delta\bar{\nu}_{1/2} = 5000$ cm$^{-1}$ and $\epsilon_{max} = 455$ M$^{-1}$ cm$^{-1}$, eq 7.[9] Scaling this spectrum as $\epsilon(\nu)\, d \ln \nu$ based on a band shape analysis by Neyhart[23] gives $\bar{\nu}_{max} = 7800$ cm$^{-1}$, $\Delta\bar{\nu}_{1/2} = 3870$ cm$^{-1}$, and $\epsilon_{max} = 385$ M$^{-1}$ cm$^{-1}$. From the spectral data and eqs 5 and 6, $\vec{M} \geq 0.011$ Å and $H_{DA} \geq 320$ cm$^{-1}$. The values cited are lower limits because delocalization has the effect of decreasing the charge-transfer distance compared to the geometric distance.

$$[(bpy)_2(Cl)Ru^{III}(pz)Ru^{II}(Cl)(bpy)_2]^{3+} \xrightarrow{h\nu} [(bpy)_2(Cl)Ru^{II}(pz)Ru^{III}(Cl)(bpy)_2]^{3+} \tag{7}$$

As illustrated for the ground state in Scheme 1, the IT "bands" for these complexes consist of three components arising from separate IT transitions.[22a] In these transitions, excitation occurs from one of three d$\pi$ levels at Ru(II) to the hole in d$\pi^5$ Ru(III).

***Scheme 1***

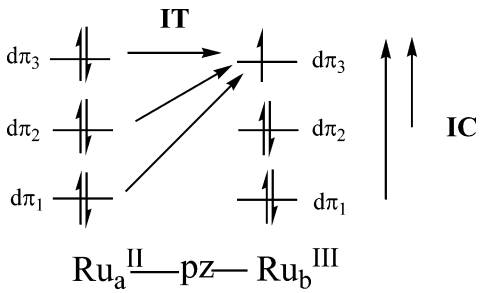


The splitting in the d$\pi$($Ru^{III}$) levels is due to low symmetry and spin−orbit coupling. These perturbations also mix the Cartesian $d_{xy}$, $d_{yz}$, and $d_{xz}$ orbitals imparting radial character along the Ru(pz)Ru axis to all three d$\pi$ orbitals.

Resolved IT components are observed in near IR spectra of related Os complexes such as $[(bpy)_2ClOs^{III}(N_2)Os^{II}Cl(bpy)_2]^{3+}$.[22a,24] In these complexes the d$\pi$−d$\pi$ energy spacings are greater due to enhanced spin−orbit coupling with $\xi(Os^{III}) \sim 3000$ cm$^{-1}$.[22a] Based on the band shape analysis by Neyhart for *cis*,*cis*-$[(bpy)_2ClRu^{II}(pz)Ru^{III}Cl(bpy)_2]^{3+}$ in $CD_3CN$ mentioned above,[23] the three components for ground state IT appear at ∼5800, ∼7600, and ∼8500 cm$^{-1}$. No attempt was made to deconvolute the excited state IT band.

As illustrated in Scheme 1, interconfigurational (IC) d$\pi \rightarrow$ d$\pi$ bands arising from the transitions

$$d\pi_{1,b}{}^2 d\pi_{2,b}{}^2 d\pi_{3,b}{}^1 \xrightarrow{h\nu} d\pi_{1,b}{}^2 d\pi_{2,b}{}^1 d\pi_{3,b}{}^2$$

$$d\pi_{1,b}{}^2 d\pi_{2,b}{}^2 d\pi_{3,b}{}^1 \xrightarrow{h\nu} d\pi_{1,b}{}^1 d\pi_{2,b}{}^2 d\pi_{3,b}{}^2$$

are also predicted to appear at low energy. In related low-symmetry complexes of Os(III) these bands appear in the near-IR at ∼4000 and ∼6000 cm$^{-1}$.[22a,24] Because of decreased spin−orbit coupling, IC bands for Ru(III) are predicted to appear at lower energy in the IR and to have greatly decreased absorptivities.[24−25]

**Electronic Coupling.** As noted above, attempts to generate *cis*,*cis*-$[(bpy)_2ClRu^{III}(pz)Ru^{II}Cl(bpy)_2](PF_6)_3$ in PMMA films to compare excited and ground state IT spectra in the same medium were unsuccessful. However, there are useful comparisons between media.

Comparison of transition moments and $H_{DA}$ values reveals that $Ru^{III}$−$Ru^{II}$ electronic coupling across pz as the bridging ligand in the ground state is comparable to $pz^{-\bullet}$ in the MLCT excited state. From the analysis in the previous section, $H_{DA}$ values are the sums of three separate orbital interactions:

(1) $H_{DA}(1)$ arising from coupling between d$\pi_3$($Ru_a^{II}$) and d$\pi_3$-($Ru_b^{III}$) by mixing with intervening pyrazine $\pi$ and $\pi^*$ orbitals,[26]

(2) $H_{DA}(2)$ arising from pyrazine-promoted mixing between d$\pi_2$($Ru_a^{II}$) and d$\pi_3$($Ru_b^{III}$), and

(3) $H_{DA}(3)$ arising from pyrazine-promoted mixing between d$\pi_1$($Ru_a^{II}$) and d$\pi_3$($Ru_b^{III}$).

The lowest energy IT band and $H_{DA}(1)$ contain information about electronic delocalization in the ground state.[22a] The two higher energy absorptions illustrated in Scheme 1 arise from

(21) Due to a lack of an appropriate actinometer in the NIR (i.e., one that can be excited with visible light near 500 nm that gives rise to a predictable spectral signature near 1500 nm), an estimation of the extinction coefficient for IT bands was calculated according to the method described in ref 18. The concentration of excited molecules at the excitation wavelength of 510 nm was calculated from the absorbance of the $[(bpy)_2(Cl)Ru^{II}(pz)Ru^{II}(Cl)(bpy)_2]^{2+}$ MLCT band in PMMA (1.15 abs units) and the extinction coefficient for $[(bpy)_2(Cl)Ru^{II}(pz)Ru^{II}(Cl)(bpy)_2]^{2+}$ in acetonitrile, $\epsilon_{510nm} = 2.6 \times 10^4$ M$^{-1}$ cm$^{-1}$ (Powers, M. J.; Meyer, T. J. *J. Am. Chem. Soc.* **1980**, *102*, 1289). The absorbance at 6880 cm$^{-1}$ was measured 30 ns after the laser flash. Based on the time-resolved emission traces, the loss of the excited state after 30 ns was ∼30%. The excited state $\epsilon$ value was estimated by correcting the measured absorbance for the amount of excited state decay, the film thickness of 0.7 mm, and Beer's law. Absorbance by the PMMA film at 6880 cm$^{-1}$ is negligible, Figure 4A. Using this method, $\epsilon_{max} \geq 970$ M$^{-1}$ cm$^{-1}$. This is a lower limit since it assumes that the excited state observed is formed with unit efficiency. A less than unit efficiency would increase the extinction coefficient.

(22) (a) Demadis, K. D.; Hartshorn, C. M.; Meyer, T. J. *Chem. Rev.* **2001**, *101*, 2655−2685 and references therein. (b) Bublitz, G. U.; Laidlaw, W. M.; Denning, R. G.; Boxer, S. G. *J. Am. Chem. Soc.* **1998**, *120*, 6068. (c) Hupp, J. T.; Dong, Y.; Blackburn, R. L.; Lu, H. *J. Phys. Chem.* **1993**, *97*, 3278−3282. (d) Creutz, C.; Newton, M. D.; Sutin, N. *J. Photochem. Photobiol., A* **1994**, *82*, 47−59. (e) Reimers, J. R.; Hush, N. S. *J. Am. Chem. Soc.* **1995**, *117*, 1302−1308. (f) Salaymeh, F.; Berhane, S.; Yusof, R.; de la Rosa, R.; Fung, E. Y.; Matamoros, R.; Lan, K. W.; Zheng, Q.; Kober, E. M.; Curtis, J. C. *Inorg. Chem.* **1993**, *32*, 3895−3908. (g) Brunschwig, B. S.; Creutz, C.; Sutin, N. *Chem. Soc. Rev.* **2002**, *31*, 168−184.

(23) Neyhart, G. A. Ph.D. Dissertation, University of North Carolina at Chapel Hill, Chapel Hill, NC, 1988.

(24) (a) Demadis, K. D.; Neyhart, G. A.; Kober, E. M.; White, P. S.; Meyer, T. J. *Inorg. Chem.* **1999**, *38*, 5948−5959. (b) Kober, E. M. Ph.D. Dissertation, University of North Carolina at Chapel Hill, Chapel Hill, NC, 1982.

(25) Hudson, A.; Kennedy, M. J. *J. Chem. Soc. A* **1969**, 1116.

***Scheme 2***

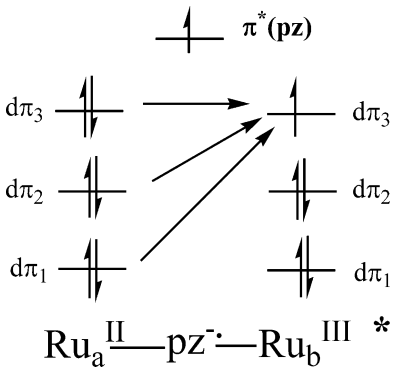


transitions with mixed IT−IC character and result in interconfigurational, d$\pi$−d$\pi$ excited states. To illustrate the point in orbital terms, the second transition illustrated in Scheme 1 is

$$d\pi_1(Ru_a^{II})^2 d\pi_2(Ru_a^{II})^2 d\pi_3(Ru_a^{II})^2 d\pi_3(Ru_b^{III})^1 \xrightarrow{h\nu} d\pi_1(Ru_a^{III})^2 d\pi_2(Ru_a^{III})^1 d\pi_3(Ru_a^{III})^2 d\pi_3(Ru_b^{II})^2$$

In this case, the mixed IT−IC transition gives an IC excited state at photoproduced $Ru_a^{III}$. $H_{DA}(2)$ and $H_{DA}(3)$ are the resonance energies arising from cross-bridge coupling in the IC excited states.

Based on this analysis, $\bar{\nu}_{max}$ for the two higher energy IT transitions illustrated in Scheme 1 is a sum of reorganization energies, $\lambda$, and the energy gaps between the ground and IC excited state, $\Delta E_{d\pi}(1)$ or $\Delta E_{d\pi}(2)$, with $\bar{\nu}_{max}\,(2) = \lambda + \Delta E_{d\pi}(1)$ and $\bar{\nu}_{max}\,(3) = \lambda + \Delta E_{d\pi}(2)$. This assumes that $H_{DA} \ll \lambda$. The reorganization energy is the sum of intramolecular ($\lambda_i$) and medium ($\lambda_o$) contributors.

A quantitative comparison between excited and ground state $H_{DA}(1)$ values cannot be made without deconvolution of the IT bands because, as noted above, they consist of three overlapping components. Nonetheless, the similarity between $H_{DA}$ values calculated from the experimental IT bands for the ground and excited state point to comparable electronic coupling between $Ru^{II}$ and $Ru^{III}$ for $pz^{-\bullet}$ and pz as bridging ligands, at least in this bpy-based coordination environment.

Even though the extent of electronic coupling is comparable, the orbital bases for electronic interaction are significantly different between the ground and excited states. In $[(bpy)_2ClRu^{III}(pz)Ru^{II}Cl(bpy)_2]^{3+}$, through-bridge electronic coupling is dominated by mixing between d$\pi$($Ru^{II}$) and $\pi$*(pz) orbitals. Mixing with bridging ligand orbitals extends d$\pi$($Ru^{II}$) orbital character across the bridge where overlap occurs with d$\pi$($Ru^{III}$).[22,26−28]

The anticipated orbital coupling scheme in $[(bpy)_2ClRu^{III}(pz^{\bullet-})Ru^{II}Cl(bpy)_2]^{2+*}$ is significantly different. As shown in Scheme 2 the excited electron occupies a d$\pi_3$-($Ru^{III}$)−$\pi$*(pz) molecular orbital. This orbital is largely $\pi$*(pz) in character but extensively mixed with d$\pi_3$($Ru^{III}$). Electronic coupling across the bridge is dominated by overlap between the d$\pi_a$($Ru^{II}$) orbitals and the mixed, metal−ligand excited-state orbital.

Based on this analysis, the observation of comparable electronic coupling in ground and excited states is coincidental given the different orbital interactions for the two. It reflects a balance between d$\pi$($Ru^{II}$)−$\pi$*(pz) mixing in the ground state and the directed character of excited-state charge transfer along the bridging ligand in the excited state.

**Medium Effects.** For the ground state IT transition in eq 7, $\Delta G^0 = 0$ in solution. In the classical limit, $\bar{\nu}_{max}$ is given by eq 8. As noted above, $\nu_{max}$ is the sum of $\lambda_i$ and $\lambda_o$.[22,27a,b,29−30]

$$\bar{\nu}_{max} = \lambda = \lambda_o + \lambda_i \tag{8}$$

In a rigid medium, $\Delta G^0 > 0$ for the IT transition because part of the surrounding medium is frozen, as are counterion placements. Following a treatment by Marcus, $\lambda_o$ can be partitioned into a frozen part, $\lambda_{oo}$, and a nonfrozen part, $\lambda_{oi}$, eq 9.[30,31]

$$\lambda_o = \lambda_{oo} + \lambda_{oi} \tag{9}$$

$\lambda_{oo}$ originates in collective, large amplitude displacements in the surrounding medium that are frozen in a rigid medium. Because they are frozen, $\lambda_{oo}$ becomes part of $\Delta G^0$ and no longer contributes to the reorganization energy.[32] $\lambda_o$ originates in single molecule rotations and lattice displacements that are not frozen.

There is an additional contribution to $\Delta G^0$ in rigid media due to the surrounding counterions with an associated reorganization energy $\lambda_{X^-}$. It is the reorganization energy arising from the charge imbalance created by the transfer of the electron without transfer of the associated counterions to their new equilibrium positions. The origin of this contribution is illustrated schematically in eq 10. It shows that in a rigid medium intervalence

$$(X^-)_2[^{2+}(bpy)_2ClRu^{III}(pz)Ru^{II}Cl(bpy)_2^{+}](X^-) \xrightarrow{h\nu} (X^-)_2[(^{+}bpy)_2ClRu^{II}(pz)Ru^{III}Cl(bpy)_2^{2+}](X^-) \tag{10}$$

transfer leads to a counterion distribution appropriate to the initial charge distribution and not the final distribution. In an equivalent fluid, ion-paired counterions would re-equilibrate by translation−rotation. In a rigid medium they are frozen.

In a rigid (frozen, fr) medium, ion pairing and the partly frozen environment create a $\Delta G^0$ difference between the initial and final mixed valence states. As shown in eq 11,

$$\Delta G^0(fr) = \lambda_{oo} + \lambda_{X^-} \tag{11a}$$

$$\bar{\nu}_{max} = (\lambda_i + \lambda_{oo} + \lambda_{oi} + \lambda_{X^-}) = (\lambda_i + \lambda_{oi} + \Delta G^0_{fr}) \tag{11b}$$

they contribute the quantities $\lambda_{oo}$ and $\lambda_X-$ to $\bar{\nu}_{max}$ for intervalence transfer with $\Delta G^0(fr) = \lambda_{oo} + \lambda_{X^-}$. The charges on the separate, constituent complexes are shown as superscripts in eq 10.

(26) (a) Broo, A.; Lincoln, P. *Inorg. Chem.* **1997**, *36*, 2544. (b) Lauher, J. W. *Inorg. Chim. Acta* **1980**, *39*, 119. (c) Broo, A.; Larsson, S. *Chem. Phys.* **1982**, *161*, 363. (d) Ondrechen, M. J.; Ko, J.; Root, L. J. *J. Phys. Chem.* **1984**, *88*, 5919. (e) Zhang, L. T.; Ko, J.; Ondrechen, M. J. *J. Phys. Chem.* **1989**, *93*, 3030. (f) Ferretti, A.; Lami, A.; Villani, G. *Inorg. Chem.* **1998**, *37*, 2799. (g) Bencini, A.; Ciofini, I.; Daul, C. A.; Ferretti, A. *J. Am. Chem. Soc.* **1999**, *121*, 11418.
(27) (a) Creutz, C. *Prog. Inorg. Chem.* **1983**, *30*, 1. (b) Callahan, R. W.; Keene, F. R.; Meyer, T. J.; Salmon, D. J. *J. Am. Chem. Soc.* **1977**, *99*, 1064. (c) Zwickel, A. M.; Creutz, C. *Inorg. Chem.* **1971**, *10*, 2395.
(28) Piepho, S. B. *J. Am. Chem. Soc.* **1988**, *110*, 6319.
(29) Chen, P.; Meyer, T. J. *Chem. Rev.* **1998**, *98*, 1439−1477.
(30) Marcus, R. A. *J. Phys. Chem.* **1989**, *93*, 3078. Marcus, R. A.; Sutin, N. *Biochim. Biophys. Acta* **1985**, *811*, 265−322. 26.
(31) (a) Brandup, J., and Immergut, E. H. *Polymer Handbook*, 3rd ed. John Wiley & Sons: New York, 1989. (b) In $CH_3CN$, $D_{op} = 1.81$ and $D_s = 36.2$. In PMMA, $D_{op} = 2.22$ and $D_s = 3.6$.
(32) Chen, P. Y.; Meyer, T. J. *Inorg. Chem.* **1996**, *35*, 5520−5524.

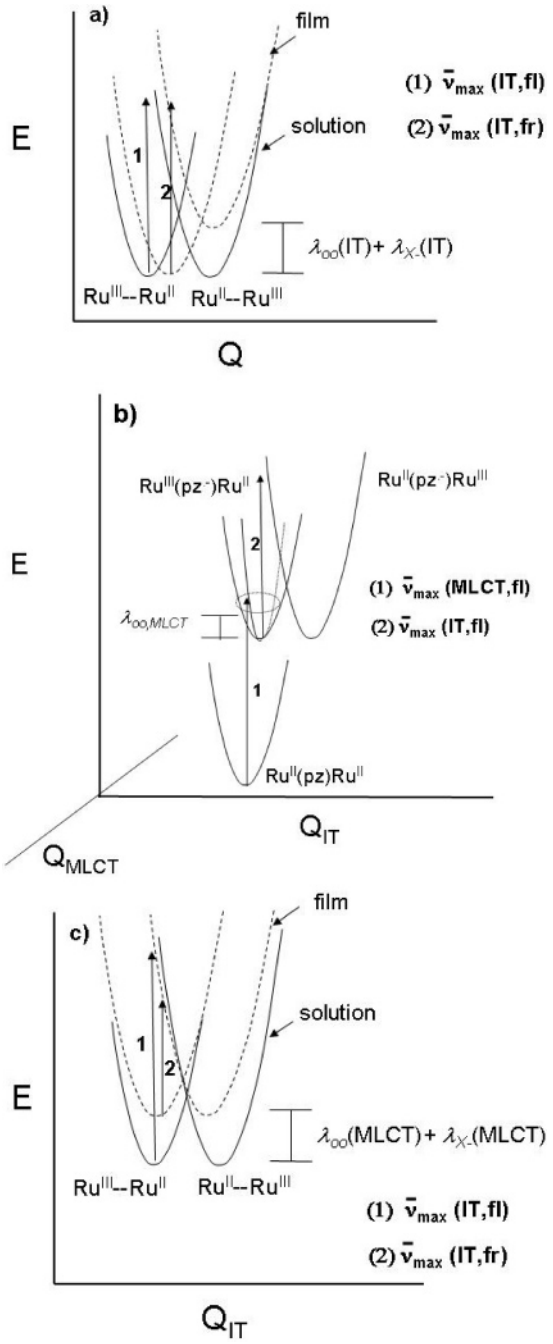


***Figure 5.*** (a) Energy coordinate curves illustrating the $Ru^{II}(pz)Ru^{III} \rightarrow Ru^{III}(pz)Ru^{II}$ (with h$\nu$) ground state IT transition in solution (—) and in a rigid (frozen) film environment ( - - - ) in the classical limit with the average mode approximation with $\bar{\nu}_{max} = \lambda = \lambda_o + \lambda_i$ (solution) and $\bar{\nu}_{max} = \lambda_{oi} + \lambda_i + \Delta G = \lambda_i + \lambda_{oi} + \lambda_{oo} + \lambda_{X^-}$ (film); see text. The fluid and frozen transitions are shown as (1) and (2), respectively. (b) As in (a) illustrating MLCT excitation in solution to create an excited-state mixed-valence complex, $Ru^{III}(pz^{-\bullet})Ru^{II}$ with excitation along coordinate $Q_{MLCT}(1)$ and intervalence transfer (IT) following excited-state relaxation along coordinate $Q_{IT}(2)$. (c) As in (b) illustrating intervalence transfer in the $Ru^{III}(pz^{-\bullet})Ru^{II}$ mixed-valence excited state in solution (1) and in $(X^-)Ru^{III}(pz^{-\bullet})Ru^{II}(X^-)$ in a rigid medium (2).

Intervalence transfers both in solution and in a comparable rigid medium are illustrated schematically in the energy-coordinate diagram in Figure 5A. This diagram utilizes the average mode approximation and assumes the classical, harmonic limit. $\bar{\nu}_{max}$ is shown as being nearly the same in both media to illustrate that the decrease in $\lambda$ in a rigid medium is compensated for by the appearance of a $\Delta G^0$ with $\Delta G^0$ ($= \lambda_{oo} + \lambda_{X^-}$) > 0.

Excited state IT is more complex because it involves two transitions, one to give the MLCT excited state and the other intervalence transfer. It is useful to consider the solution case in eq 12 first.

$$[(bpy)_2ClRu^{II}(pz)Ru^{II}Cl(bpy)_2]^{2+} \xrightarrow[MLCT]{h\nu} [(bpy)_2ClRu^{III}(pz^{-\bullet})Ru^{II}Cl(bpy)_2]^{2+} \xrightarrow[IT]{h\nu} [(bpy)_2ClRu^{II}(pz^{-\bullet})Ru^{III}Cl(bpy)_2]^{2+*} \quad (12)$$

As shown in Figure 5B, excited state IT involves two separate sets of coupled modes. One set is coupled to the initial MLCT transition. The second is coupled to the excited state IT transition.

For MLCT absorption, $\bar{\nu}_{max}$(MLCT) is the sum of the free energy of the equilibrated excited state above the ground state, $\Delta G^0_{MLCT}$, and the reorganization energy between ground and excited states, $\lambda_o$(MLCT) + $\lambda_i$(MLCT), eq 13, neglecting ion pairing. The MLCT label is added to specify the MLCT character of the transition.

Following MLCT excitation, intervalence transfer is observed at $\bar{\nu}_{max}$(IT), eq 14. The labels fl and fr in eqs 13−15 denote that this is the result predicted in either fluid or frozen (rigid) media. Given the ~20 ns time resolution of the TRNIR measurement, intervalence transfer is measured on the thermally equilibrated MLCT excited state.

$$\bar{\nu}_{max}(MLCT,fl) = \Delta G^0_{MLCT,fl} + \lambda_o(MLCT) + \lambda_i(MLCT) \quad (13)$$

$$\bar{\nu}_{max}(IT,fl) = \lambda_o(IT) + \lambda_i(IT) \quad (14)$$

$$\bar{\nu}_{max}(MLCT,fr) = \Delta G^0_{MLCT,fl} + \lambda_o(MLCT) + \lambda_i(MLCT) + \lambda_{X^-} \quad (15)$$

For $(PF_6)[(bpy)_2ClRu^{III}(pz^{-\bullet})Ru^{II}Cl(bpy)_2](PF_6)$ in PMMA, $\bar{\nu}_{max}$ (MLCT) is given by eq 15 which includes an additional contribution from reorganization of counterions compared to solution. After excitation and equilibration the energy of the MLCT state is increased compared to a comparable fluid by $\lambda_{oo}$(MLCT) + $\lambda_{X^-}$(MLCT), eq 16.

$$\Delta G^0_{ES,fr} = \Delta G^0_{ES,fl} + \lambda_{X^-}(MLCT) + \lambda_{oo}(MLCT) \quad (16)$$

Excited-state intervalence transfer in $(PF_6)[(bpy)_2ClRu^{III}(pz^{-\bullet})Ru^{II}Cl(bpy)_2](PF_6)$ in PMMA is illustrated in eq 17. For this transition, the $\lambda_{oo}$ part of the medium reorganization energy and $\lambda_{X^-}$ are frozen in the configurations that existed before MLCT excitation, their configurations in the ground state.

$$(PF_6^-)[^+(bpy)_2ClRu^{II}(pz)Ru^{II}Cl(bpy)_2^+](PF_6^-) \xrightarrow[MLCT]{h\nu} (PF_6^-)[^{*2+}(bpy)_2ClRu^{III}(pz^{-\cdot})Ru^{II}Cl(bpy)_2^+](PF_6^-) \xrightarrow[IT]{h\nu} (PF_6^-)[^+(bpy)_2ClRu^{II}(pz^{-\cdot})Ru^{III}Cl(bpy)_2^{2+*}](PF_6^-) \quad (17)$$

Following MLCT excitation and relaxation, they remain symmetrical. As noted in eq 16, this has the effect of increasing the free energy of the excited state relative to a comparable fluid. *However, since $\lambda_{oo}$ and $\lambda_{X^-}$ are frozen, they do not contribute to the IT barrier in PMMA. This results in a decrease in $\bar{\nu}_{max}$(IT) in a rigid medium relative to a comparable fluid, eq 18.*

$$\bar{\nu}_{max}(\mathrm{IT,fr}) = \lambda_{oi}(\mathrm{IT}) + \lambda_i(\mathrm{IT}) \qquad (18)$$

IT absorptions in the two media are illustrated in the energy-coordinate diagram in Figure 5c.

**Medium Effects, Comparisons.** Although one is rigid and the other is fluid, PMMA and $CH_3CN$ are similar in their influence on charge transfer absorption. $\bar{\nu}_{max}$ for $d\pi(Ru^{II}) \rightarrow \pi^*(pz)$ MLCT absorption in *cis,cis*-$[(bpy)_2ClRu^{II}(pz)Ru^{II}Cl(bpy)_2](PF_6)_2$ occurs at $\bar{\nu}_{max} = 520$ nm (19 200 $cm^{-1}$) in PMMA and at 508 nm (19 700 $cm^{-1}$) for *cis,cis*-$[(bpy)_2ClRu^{II}(pz)Ru^{II}Cl(bpy)_2]^{3+}$ in $CD_3CN$.[9]

As noted in the previous section, IT absorption by $[(bpy)_2ClRu^{III}(pz)Ru^{II}Cl(bpy)_2]^{3+}$ in $CD_3CN$ also occurs at higher energy (7700 vs 6880 $cm^{-1}$) than the excited state in PMMA and the absorption manifold is broader (5000 vs 3740 $cm^{-1}$). Both are predicted qualitatively by the analysis in the previous section. From eqs 14 and 18 the difference in energy between fluid and frozen media is given by eq 19. Although differences in $\lambda_i$ and $\lambda_{oi}$ contribute to $\Delta\bar{\nu}_{max} = 820$ $cm^{-1}$, $\lambda_{oo}$ may be the major contributor. $\lambda_{oi}$ is typically small, as are percentage changes in $\lambda_i$ between media.[33]

$$\Delta\bar{\nu}_{max}(\mathrm{IT}) = \bar{\nu}_{max}(\mathrm{IT,fl}) - \bar{\nu}_{max}(\mathrm{IT,fr}) = (\lambda_{i,fl} - \lambda_{i,fr}) + (\lambda_{oi,fl} - \lambda_{oi,fr}) + \lambda_{oo}(\mathrm{IT}) \qquad (19)$$

A decrease in bandwidth is also predicted since, in the classical, harmonic oscillator limit, $\Delta\bar{\nu}_{1/2}$ is related to $\bar{\nu}_{max}$ as shown in eq 20.[34] As noted above, analysis and comparison of IT band shapes by using eqs 19 and 20 are complicated since the absorption manifolds consist of three overlapping bands.

$$\Delta\bar{\nu}_{1/2} = (2310 \cdot \bar{\nu}_{max})^{1/2} \qquad (\text{at } 25\ ^\circ\mathrm{C}) \qquad (20)$$

Contributions to $\Delta\bar{\nu}_{max}$(IT) from $\lambda_o$ in the two media can be estimated from classical dielectric continuum theory. In the limit that electron transfer occurs between non-interpenetrating spheres of radii $a_1$ and $a_2$ separated by distance $d$, $\lambda_o$ is predicted to vary as

$$\lambda_o = e^2\left(\frac{1}{2a_1} + \frac{1}{2a_2} - \frac{1}{d}\right)\left(\frac{1}{D_{op}} - \frac{1}{D_s}\right)$$

with $D_{op}$ and $D_s$ as the optical and static dielectric constants.[35−40] More elaborate treatments are available,[41] but based on this result and the known dielectric constants,[31] $\lambda_o$ is predicted to be ~66% less in PMMA. This result is qualitatively consistent with the decreases in $\bar{\nu}_{max}$(IT) and $\Delta\bar{\nu}_{1/2}$ in PMMA.

**Intramolecular Electron Transfer.** The classical barriers to thermal intramolecular electron transfer are different in fluid, eq 21, and frozen media, eq 22.

$$[(bpy)_2(Cl)Ru^{III}(pz)Ru^{II}(Cl)(bpy)_2]^{3+} \rightarrow [(bpy)_2(Cl)Ru^{II}(pz)Ru^{III}(Cl)(bpy)_2]^{3+} \qquad (21)$$

$$(X^-)_2[^{2+}(bpy)_2ClRu^{III}(pz)Ru^{II}Cl(bpy)_2{}^+](X^-) \rightarrow (X^-)_2[^{+}(bpy)_2ClRu^{II}(pz)Ru^{III}Cl(bpy)_2{}^{2+}](X^-) \qquad (22)$$

The respective free energies of activation, $\Delta G^*$(fl), and $\Delta G^*$(fr), are given in eqs 23 and 24 with the $\lambda$'s being those appropriate for intervalence transfer (IT).[34]

$$\Delta G^*_{fl}(\mathrm{IT}) = \frac{\lambda}{4} = \frac{(\lambda_i + \lambda_{oi} + \lambda_{oo})}{4} \qquad (23)$$

$$\Delta G^*_{fr}(\mathrm{IT}) = \frac{(\lambda + \Delta G^0)^2}{4\lambda} = \frac{(\lambda_{oi} + \lambda_i + \lambda_{oo} + \lambda_{X^-})^2}{4(\lambda_i + \lambda_{oi})} : \quad (\Delta G = \lambda_{oo} + \lambda_{X^-}) \qquad (24)$$

Assuming that the $\lambda$'s, $\lambda_i$, $\lambda_{oo}$, and $\lambda_{oi}$, are comparable in the two media, the $\Delta G^*$ values are related by

$$\Delta G^*_{fr} \approx \left(1 + \frac{\lambda_{oo} + \lambda_{X^-}}{\lambda_i + \lambda_{oi}}\right)\Delta G^*_{fl} \qquad (25)$$

This shows, at least qualitatively, that the barrier to intramolecular electron transfer in a rigid medium is greater than that in a comparable fluid because $\lambda_{oo} + \lambda_{X^-}$ ($= \Delta G^0$(fr)) is > 0 increasing the driving force. This is a general result showing that in order to achieve comparable reaction rates for electron transfer in rigid media, as in solution a more favorable driving force is required.[29,44,4542−45]

By contrast the barrier to excited-state electron transfer in a rigid medium, e.g.,

$$(X^-)[^{*2+}(bpy)_2ClRu^{III}(pz^{-})Ru^{II}Cl(bpy)_2{}^+](X^-) \longrightarrow (X^-)[^{+}(bpy)_2ClRu^{II}(pz^{\cdot})Ru^{III}Cl(bpy)_2{}^{2+*}](X^-)$$

is *less* than that in solution with $\Delta G^*_{fr,ES} < \Delta G^*_{fl,ES}$. Assuming comparable reorganization energies, the two are related as shown in eq 26.

$$\Delta G^*_{fr,ES} = \lambda_{oi} + \lambda_i = \Delta G^*_{fl,ES} - \lambda_{oo} \qquad (26)$$

This is also a general result. Once the initial increase in activation for electron transfer in a rigid medium is overcome, in this case by charge-transfer excitation, subsequent electron-transfer hopping between sites occurs with a decreased activation barrier.

(33) Watts, R. J.; Missimer, D. *J. Am. Chem. Soc.* **1978**, *100*, 5350.
(34) Hush, N. S. *Prog. Inorg. Chem.* **1967**, *8*, 391.
(35) Sutin, N. *Acc. Chem. Res.* **1982**, *15*, 275.
(36) Brunschwig, B. S.; Sutin, N. *Coord. Chem. Rev.* **1999**, *187*, 233.
(37) Newton, M. D. *Chem. Rev.* **1991**, *91*, 767−792.
(38) Jortner, J.; Bixon, M. *Ber. Bunsen-Ges. Phys. Chem.* **1995**, *99*, 296.
(39) Marcus, R. A. *Annu. Rev. Phys. Chem.* **1966**, *15*, 155.
(40) Hush, N. S. *Prog. Inorg. Chem.* **1967**, *8*, 391.
(41) Dogonadze, R. R.; Kuznetsov, A. M. *Prog. Surf. Sci.* **1975**, *6*, 1.
(42) Marcus, R. A. *Rev. Mod. Phys.* **1993**, *65*, 599.
(43) Matyushov, D.; Schmid, R. *J. Phys. Chem.* **1994**, *98*, 5152−5159. Matyushov, D. *Mol. Phys.* **1993**, *79*, 795. Matyushov, D. *Chem. Phys.* **1993**, *174*, 199−218. Basilevsky, M. V.; Rostov, I. V.; Newton, M. D. *Chem. Phys.* **1998**, *232*, 189−199. Newton, M. D.; Basilevsky, M. V.; Rostov, I. V. *Chem. Phys.* **1998**, *232*, 201−210.
(44) Chen, P. Y.; Meyer, T. J. *Inorg. Chem.* **1996**, *35*, 5520−5524.
(45) Jones, W. E., Jr.; Chen, P. Y.; Meyer, T. J. *J. Am. Chem. Soc.* **1992**, *114*, 387−388.

**Acknowledgment.** This work was supported at the University of North Carolina at Chapel Hill by the Chemical Sciences, Geosciences and Biosciences Division, Office of Basic Energy Sciences, U.S. Department of Energy under Grant Number DE-FG02-06ER15788. Additional support for D.W.T. for a Postdoctoral Research Fellowship from the Natural Science and Engineering Research Council of Canada (NSERC) and for D.M.D. from a Director's Funded Postdoctoral Fellowship at Los Alamos National Laboratory is also gratefully acknowledged.

**Note Added after ASAP:** Errors in the paper were corrected for the version published July 24, 2007.

JA068074J